BB

CEA/SACLAY
DSM

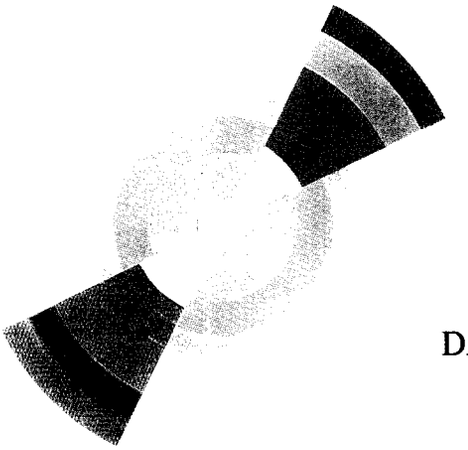

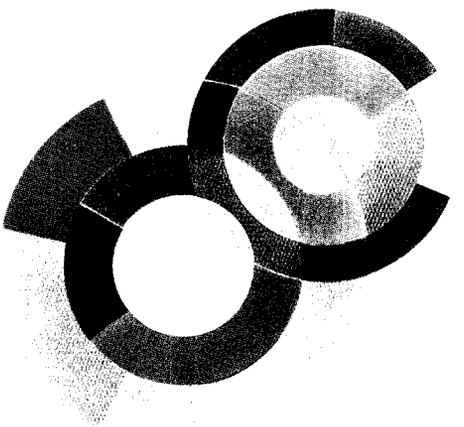

DAPNIA/SPhN-96-43 11/1996

A hot expanding source in 50 A.MeV Xe+Sn central reactions

N. Marie, R. Laforest, R. Bougault, J.P. Wieleczko, D. Durand, Ch.O. Bacri, J.F. Lecolley, F. Saint-Laurent, G. Auger, J. Benlliure, E. Bisquer, B. Borderie, R. Brou, J.L. Charvet, A. Chbihi, J. Colin, D. Cussol, R. Dayras, E. De Filippo, A. Demeyer, D. Doré, P. Ecomard, P. Eudes, D. Gourio, D. Guinet, P. Lautesse, J.L. Laville, A. Le Fèvre, T. Lefort, R. Legrain, O. Lopez, M. Louvel, V. Métivier, L. Nalpas, A. Ouatizerga, M. Parlog, J. Péter, E. Plagnol, A. Rahmani, T. Reposeur, M.F. Rivet, E. Rosato, S. Salou, M. Squalli, J.C. Steckmeyer, B. Tamain, L. Tassan-Got, E. Vient, C. Volant.

DAPNIA

Département d'**A**strophysique, de Physique des **P**articules, de Physique **N**ucléaire et de l'**I**nstrumentation **A**ssociée
CEA/Saclay F-91191 Gif-sur-Yvette Cédex

Couverture : Sylvie Cabin et Marc Sauvage

Submitted to the Physics Letters B

A hot expanding source in 50 A.MeV Xe+Sn central reactions ⋆

N. Marie [a,1], R. Laforest [b,2], R. Bougault [b], J.P. Wieleczko [a], D. Durand [b], Ch.O. Bacri [c], J.F. Lecolley [b], F. Saint-Laurent [a], G. Auger [a], J. Benlliure [a], E. Bisquer [e], B. Borderie [c], R. Brou [b], J.L. Charvet [d], A. Chbihi [a], J. Colin [b], D. Cussol [b], R. Dayras [d], E. De Filippo [d], A. Demeyer [e], D. Doré [c], P. Ecomard [a], P. Eudes [f], D. Gourio [f], D. Guinet [e], P. Lautesse [e], J.L. Laville [f], A. Le Fèvre [a], T. Lefort [b], R. Legrain [d], O. Lopez [b], M. Louvel [b], V. Métivier [f], L. Nalpas [d], A. Ouatizerga [c], M. Parlog [c], J. Péter [b], E. Plagnol [c], A. Rahmani [f], T. Reposeur [f], M.F. Rivet [c], E. Rosato [b], S. Salou [a], M. Squalli [c], J.C. Steckmeyer [b], B. Tamain [b], L. Tassan-Got [c], E. Vient [b], C. Volant [d]

[a] *GANIL (DSM-CEA/IN2P3-CNRS), B.P.5027, F-14021 Caen cédex, France*

[b] *LPC Caen (IN2P3-CNRS/ISMRA et Université), F-14050 Caen cédex, France*

[c] *IPN Orsay (IN2P3-CNRS), F-91406 Orsay cédex, France*

[d] *CEA DAPNIA-SPhN, CE Saclay, F-91191 Gif sur Yvette, France*

[e] *IPN Lyon (IN2P3-CNRS/Université), F-69622 Villeurbanne cédex, France*

[f] *SUBATECH (IN2P3-CNRS/Université), F-44072 Nantes cédex 03, France*

Abstract

The INDRA multidetector has been used to study multifragmentation processes in central collisions for the Xe+Sn reaction at 50 A.MeV. A single isotropic source formed at an excitation energy of 12 A.MeV exhausting most of the emitted charged products has been isolated in such collisions. The fragment kinetic energy spectra indicate a fast disintegration of the system with a radial collective motion of about 2 A.MeV. The light charged particle characteristics within this scenario are also discussed.

Preprint submitted to Elsevier Science *15 October 1996*

The predominant decay mode of highly excited nuclei is the disassembly into several intermediate sized fragments [1]. The understanding of this multifragmentation process has triggered a blooming of theoretical works which differ in the degrees of freedom involved [1,2], but the physics which drives the phenomenon is not yet well delineated. In this context, exploration of multifragmentation in very central nucleus-nucleus collisions is fundamental since compressed matter is expected to be created early on in the collision. Therefore such investigations might reveal whether compression induces a specific pattern for multifragmentation and help to disentangle true dynamical mechanisms from trivial phase-space effects [3]. Recent analyses of the kinetic energy of fragments or light particles [4–9] [10–16] have suggested that a significant part of the available energy is converted into collective motion of matter. In this letter we present evidence for radial collective motion of the fragments emitted during the multifragmentation of a single source formed in central collisions of the quasi-symmetric Xe+Sn system at 50 A.MeV.

The experiment was performed using a 50 A.MeV ^{129}Xe beam with an intensity of 5.10^7 pps delivered by the GANIL facility. This beam impinged on a 350 μg/cm^2 thick self-supporting ^{nat}Sn target. Charged products were detected with the INDRA detector which covers the laboratory angles $2^\circ \leq \Theta_{lab} \leq 176^\circ$ and has a geometrical acceptance of 90% of 4π. Charged particles were identified in atomic number with a resolution better than one unit up to $Z \approx 60$; isotopic separation for $Z \leq 4$ was achieved up to about 200 A.MeV. Absolute energy calibrations are estimated to be accurate to within 5%. Identification thresholds evolve from 0.7 A.MeV to 1.7 A.MeV as the atomic number increases from 1 to around 60. More details can be found in refs. [17–19]. During the experiment, events were recorded when at least four INDRA detector elements were triggered. Some data were registered with a triggering level of one. A comparison between the two sets of data indicates no influence of the trigger on the class of events discussed here.

To ensure a better control of the origin of the reaction products, only almost complete events are selected. This is done by imposing for each event two criteria : (i) the sum of the detected charges exceeds 80% of the charge of the combined system (charge conservation); (ii) the sum of the products of the charge and the parallel-velocity of each particle exceeds 80% of the product of the projectile charge and its velocity (pseudo linear momentum conservation). Events satisfying such requirements represent about 6% of the reaction cross-section and correspond to collisions producing the largest number of charged reaction products.

---

* Experiment performed at Ganil

[1] present address : Texas A&M University, College Station, USA.

[2] present address : AECL, Chalk River Laboratories, Chalk River, Canada.

As we want to address multifragmentation processes of nuclear systems formed in very central collisions, an obvious but crucial prerequisite is to isolate a data sample for which contributions from noncentral collisions are strongly suppressed. Moreover, we know from previous studies [20,21] that the dominant reaction process for symmetric and nearly symmetric systems around the Fermi energy are binary dissipative collisions accompanied by a dynamical (mid-rapidity) emission of particles. To gain more insight on the topology of the selected events we have performed an event by event shape analysis based on the 3-dimensional kinetic energy tensor [22–24] calculated in the center of mass (c.m) reference frame. In order to minimize possible secondary emission and preequilibrium perturbation, only fragments with $Z \geq 3$ were included in the calculation of the tensor. The kinetic energy event shape is approximated by an ellipsoid, the orientation of which in space is given by the three eigenvectors extracted from the diagonalization of the tensor. In the present case, we have chosen as the centrality selector the value of the angle Θ_f (defined between 0 and 90 degrees) between the beam axis and the eigenvector associated with the largest eigenvalue. For an isotropic emission from a single source there is no privileged direction for the major axis of the ellipsoid, thus the $d\sigma/d(cos\Theta_f)$ distribution is flat and independent of the multiplicity involved. On the other hand, the deexcitation pattern from binary collisions induces an elongated shape of the event with a finite value of Θ_f, with the major axis close to that of the beam direction for noncentral collisions.

The experimental $d\sigma/d(cos\Theta_f)$ distribution of the exclusive events is strongly forward peaked and becomes roughly flat for $\Theta_f \geq 60°$. For small Θ_f, the overall properties of events are typical of those of a mechanism where the colliding system retains a strong memory of the entrance channel. In Fig. 1, we present several clues which demonstrate that a selection of events for which $\Theta_f \geq 60°$ retains events from a unique source formed at small impact parameters. Fig. 1a shows the two-dimensional plot of the atomic number of each fragment versus its velocity along the ellipsoid main axis. Since most of the yield is located at the velocity of the c.m, a large part of the initial relative kinetic energy is transformed into other degrees of freedom. Furthermore, we have checked the centrality of the selected events by means of the particle-particle azimuthal correlations [25]. The correlation function for relative azimuthal angles between two alpha particles emitted from $\Theta_{lab} = 4.5°$ to $\Theta_{lab} = 110°$ (where the azimuthal angle acceptance of the INDRA moduli is constant) is reported in Fig. 1b. The flatness of the correlation function is a strong indication of small impact parameters. Furthermore, we have examined the angular dependence of the emission of fragments and light charged particles (lcp). The shape, as well as the intensity of the kinetic energy spectra, of the detected fragments are independent of their angle, and so indicate that the fragments are isotropically emitted. This is shown by the two oxygen energy spectra presented in Fig. 1c for a forward ($cos\Theta_{cm} \geq 0.5$) and a perpendicular ($-0.25 \leq cos\Theta_{cm} \leq 0.25$) emission in the c.m. Similar conclusions are

obtained for the spectra measured in directions parallel and perpendicular to the main axis of the ellipsoid. For lcp, the $d\sigma/d(cos\Theta_{cm})$ distribution is flat over the $60° \leq \Theta_{cm} \leq 120°$ angular domain reflecting an isotropic emission from a source moving at the c.m velocity. However, deviations from isotropy are clearly observed for the lcp emitted in forward and backward directions. This is shown through a comparison of the kinetic energy spectra for alpha-particles (Fig. 1d) measured at $cos\Theta_{cm} \geq 0.5$ and $-0.25 \leq cos\Theta_{cm} \leq 0.25$. This excess of particles at forward and backward angles corresponds to remnants of the entrance channel dynamics.

Since it is difficult to reject safely, on an event by event basis, the anisotropic component, we have deduced the overall properties of the isotropic source by taking into account all the fragments and twice the number of lcp emitted in the range $60° \leq \Theta_{cm} \leq 120°$ (Table 1). The measured isotropic component exhausts 90% of the total detected charges. The size of the isotropic source represents 79% of the charge of the combined system. Simulations have shown that the missing charge is preferentially associated with the anisotropic component. These features support the conclusion that events selected by means of largest values of Θ_f are strongly dominated by a mechanism where a single source of fragments is formed in 50 A.MeV Xe+Sn central collisions. It is remarkable that a substantial part of the isotropic source is observed as fragments. With an average multiplicity of 7 fragments, the average size of the largest three fragments is 15, 10 and 8. These features are strong indications that the regime of multifragmentation has been reached. By means of the calorimetry method [26] applied to all detected fragments and twice the lcp associated to the isotropic source, we have estimated that the stored excitation energy is about 12 A.MeV. The measured cross-section is about 6 mb for $cos\Theta_f \leq 0.5$. This value should be multiplied by 2 to take into account flow angles below 60°, yielding 12 mb. An estimate of the detector efficiency gives a correction factor of about 2 to 3.

Table 1

Mean characteristics for the isotropic source and for the total detected species. The light charged particle part of the isotropic source has been extrapolated.

Sum of charges for	Fragments	H	He	Total
isotropic component	51	13 (6.5x2)	18 (9x2)	82
total	51	16	23	90

One important aspect is the nature of the excitation energy stored in the system. We have addressed this question by means of the analysis of the kinetic energy distributions of the charged products. In Fig. 2a we report, for collisions with $\Theta_f \geq 60°$, the Z dependence of the mean values of the c.m kinetic energy spectra $< E_{cm} >$, of all the fragments with $3 \leq Z \leq 23$ (filled circles). Beyond vanadium, the statistics are too poor to safely extract a mean value.

The mean kinetic energy increases steadily from about 60 MeV for lithium up to a maximum value of about 110 MeV for aluminium and then stays roughly constant. Integrating over the restricted domain $70° \leq \Theta_{cm} \leq 110°$ (open circles) does not affect this behaviour. Thus, the overall trend, visible in Fig. 2a, stays remarkably stable regardless of the changes in the conditions chosen for the analysis. To investigate to what extent the trend for $< E_{cm} >$ reflects the role of the largest fragment in each event we have built separate spectra for them (Fig. 2b) and for other fragments (Fig. 2c). Whereas the trend for the largest fragment does not depend on its own selection, the mean kinetic energy $< E_{cm} >$ increases with Z for the other fragments. It is worth noting that for any given size, the mean kinetic energy is significantly smaller when the fragment is the largest in the event. This is the first time one sees clearly the details of the kinetic properties of the fragments.

Seven fragments isotropically emitted from a 12 A.MeV source and the increase of the mean kinetic energy as a function of the charges is certainly not consistent with a statistical sequential emission scenario. Thus for a quantitative interpretation of the experimental results we have performed calculations with a phenomenological model (SIMON) of fast disassembly [27]. In this model, the initial source is sampled to give a fixed number (N) of primary fragments (hereafter called prefragments) whose sizes are randomly chosen with the constraint that they are greater than a given minimal value. These prefragments are then distributed in space by imposing a spherical breaking configuration as compact as possible with a 2 fm minimal distance between their surfaces. This minimal distance leads to a mean density of about 1/3 normal nuclear matter density once a collection of initial configuration is considered. The initial momenta of the prefragments take into account, the Coulomb and thermal motions and an eventual expansion effect is mimicked with an initial selfsimilar velocity. The remaining amount of excitation energy is dissipated through secondary deexcitation of the prefragments within a series of sequential binary breakups [28]. The simulated events are filtered through the experimental device and analyzed as data. The calculations, presented here, correspond to a disintegration of an excited gold nucleus. The number (N=6) and the minimal size (A=10) of the prefragments have been determined to reasonably reproduce the experimental multiplicity and elemental distributions as well as the mean size of the largest three fragments.

In a first step of the analysis we compared the measured $< E_{cm} >$ to the prediction of the model without expansion effect. A calculation assuming a 12 A.MeV excitation energy as deduced from the experimental data is unable to reproduce the features of the elemental distributions. To reproduce these distributions, it is necessary to lower the excitation energy down to 10 A.MeV. However this pure thermal scenario clearly fails to explain the kinematical observables. The calculated mean energies are systematically too low (Fig. 2a). Furthermore, the shape of the E_{cm} spectra are not reproduced, as is shown

for $Z = 8$ in Fig. 2d. These disagreements illustrate the need for an additional motion to be superimposed onto a thermal plus Coulomb scenario. Indeed a clear improvement is observed when part of the total excitation energy is stored in a collective radial mode ($< E_r >$). The best agreement is obtained when an average collective radial energy, $< E_r > = 2$ A.MeV, is removed out of the 12 A.MeV total excitation energy. The predictions are presented in Fig. 2. For $Z \leq 13$ the $< E_{cm} >$ and its Z dependence are remarkably reproduced (Fig. 2a) as well as the shape of the energy distribution (Fig. 2d for oxygen). However, the calculated $< E_{cm} >$ continuously increases for $Z \geq 13$ in contradiction with the experimental saturation. As we know from the above experimental event by event analysis that the largest fragment dominates the mean energy profile for the highest Z, we have applied the unfolding procedure to the simulated events (Fig. 2b and 2c). The calculation is now consistent with the data regardless of the charge when the largest fragment in each event is excluded (Fig. 2c). This result suggests a better sensitivity to the collective motion when one concentrates on fragments excluding the largest one and the simulation with $< E_r > = 1$ A.MeV (3 A.MeV) under- (over-) estimates the experimental values by 25%. On the other hand, the average kinetic energy of the largest fragments is overpredicted (Fig. 2b). This is presumably due to a badly handled determination of the location of the largest fragment in the simulated breaking configuration. Conversely, these details on the kinetic properties of the fragments may provide valuable information on the distribution of matter in the multifragmentating system. Finally, we have checked that the value of $< E_r >$ remains valid against changes of the initial characteristics of the source (size and excitation energy) giving reasonable agreement for elemental and multiplicity experimental distributions.

The interpretation of the results relies on the fragment characteristics. Therefore, it could correspond to a snapshot of the disintegration process. Indeed, a unique value of 2 A.MeV collective energy fails to reproduce correctly the lcp average kinetic energy (Fig. 3). The calculation predicts an increase of the mean c.m energy with the mass of the lcp. On the contrary, the data (selected over $70° \leq \Theta_{cm} \leq 110°$) present a roughly constant value for deuterons, tritons and alpha-particles and a clear dependence on the isospin for A=3. Only the c.m energy mean values of alpha-particles and tritons match with the calculation. Since, in the calculation, the light particles are exclusively produced by secondary emissions , the quoted discrepancies could reflect peculiar steps of the whole disintegration process and the alpha-particles would be emitted mainly in the final stage and the protons at the beginning. The difficulty of unfolding the different emission steps out of the complex behaviour as shown in Fig. 3 does not allow to conciliate the kinetic information from both lcp and fragments. Due to this possibly complex disintegration a direct extraction of an eventual compression energy is difficult and a comparison with published results remains, at this time, problematic. Nevertheless, the very high kinetic energy observed for ^3He in Fig. 3 (reported also in [12,13,30] and quoted as

the "^3He puzzle") could probe the very first instant of the disassembly and inform us of the density reached in the formed system.

In conclusion, we have isolated for very central 50 A.MeV Xe+Sn collisions, a source which disintegrates isotropically (12 mb). This source corresponds to roughly the whole system. A small number of light particles do not participate in the source formation and correspond to a forward/backward anisotropic process. The disintegration pattern of the 12 A.MeV excited source corresponds definitively to a multifragmentation process where half of the total charge remains as fragments ($Z \geq 3$). By means of a phenomenological model, we found evidence for an additional collective motion in order to explain the kinematical observables for the fragments. A good sensitivity for the value of this mean collective energy is obtained once the largest fragment in each event is excluded. This mean collective energy corresponds to 17% of the total available kinetic energy. Moreover, it turns out that the measured kinetic energy of the heaviest fragment imposes strong constraints on the geometry involved in the multifragmentation process. Whether or not the measured collective energy is directly connected to compression effects or partly due to a thermal radial flow [5,29] needs further investigation. A quantitative analysis of all features of the observed multifragmenting source, especially the light charged particles, has to be done to study the possible role of the expansion in the decay properties.

We are grateful to M. Mac Cormick for her careful reading of the manuscript. The work of R.L. has been supported by NSERC-Canada.

References

[1] See, for instance, L.G. Moretto and G.J. Wozniak, Annu. Rev. Nucl. Part. Sci. (1993) 379, and references quoted therein.

[2] D.H.E. Gross, Rep. Prog. Phys. 59 (1990) 605.

[3] D.H.E. Gross, Phys. Scr. T 5 (1983) 213.

[4] H.W. Barz et al., Nucl. Phys. A 531 (1991) 453.

[5] R.T. de Souza et al., Phys. Lett. B 300 (1993) 29.

[6] W. Bauer et al., Phys. Rev. C 47 (1993) R1838.

[7] R. Bougault et al., XXXII Intern. Winter Meeting on Nuclear Physics (Bormio, January 1994), ed. I. Iori.

[8] S.C. Jeong et al., Phys. Rev. Lett. 72 (1994) 3468.

[9] W.C. Hsi et al., Phys. Rev. Lett. 73 (1994) 3367.

[10] D. Heuer et al., Phys. Rev. C 50 (1994) 1943.

[11] F. Schussler et al., Nucl. Phys. A 584 (1995) 704.

[12] G. Poggi et al., Nucl. Phys. A 586 (1995) 755.

[13] M.A. Lisa et al., Phys. Rev. Lett. 75 (1995) 2662.

[14] R. Kotte et al., Phys. Rev. C 51 (1995) 2686.

[15] S.C. Jeong et al., to be published in Nucl. Phys. A.

[16] J.C. Steckmeyer et al., Phys. Rev. Lett. 76 (1996) 4895.

[17] J. Pouthas et al., Nucl. Instrum. Methods A 357 (1995) 418.

[18] J.C. Steckmeyer et al., Nucl. Instrum. Methods A 361 (1995) 472.

[19] J. Pouthas et al., Nucl. Instrum. Methods A 369 (1996) 222.

[20] J. Péter et al., Nucl. Phys. A 593 (1995) 95.

[21] V. Métivier et al., XXXIII Intern. Winter Meeting on Nuclear Physics (Bormio, January 1995), ed. I. Iori.

[22] J. Cugnon and D. L'Hote, Nucl. Phys. A 397 (1983) 519.

[23] J.F. Lecolley et al., Phys. Lett. B 325 (1994) 317.

[24] M. D'Agostino et al., Phys. Lett. B 368 (1996) 259.

[25] L. Phair et al., Nucl. Phys. A 564 (1993) 453.

[26] D. Cussol et al., Nucl. Phys. A 541 (1993) 298.

[27] O. Lopez et al., Phys. Lett. B 315 (1993) 34.

[28] L. Moretto et al., Nucl. Phys. A 247 (1975) 211.

[29] W.A. Friedman, Phys. Rev. C 42 (1990) 667.

[30] K.G.R. Doss et al., Mod. Phys. Lett. A 3 (1988) 849.

Fig. 1. Characteristics of very central events ($\Theta_f \geq 60°$).
a) Charge of each fragment versus its velocity along the ellipsoid mean axis. The z-scale is logarithmic. b) Azimuthal correlation between alpha-particles emitted in the angular range $\Theta_{lab} = 4.5°$ to $\Theta_{lab} = 110°$. c) Oxygen c.m energy spectra for $cos\Theta_{cm} \geq 0.5$ (histogram) and for $-0.25 \leq cos\Theta_{cm} \leq 0.25$ (open circles). d) Alpha-particle c.m energy spectra for $cos\Theta_{cm} \geq 0.5$ (histogram) and for $-0.25 \leq cos\Theta_{cm} \leq 0.25$ (open circles).

Fig. 2. Kinetic energy characteristics of the fragments for very central events ($\Theta_f \geq 60°$) in the c.m. The experimental data are shown by circles (open and filled, see text). The result of a phenomenological multifragmentation model with (grey area for 2a,b,c) and without (white area for 2a) collective radial motion are presented. The thickness of the areas represents the error on the mean value. a) Average kinetic energies of the fragments as a function of their Z. b) Average kinetic energy of the largest fragment in each event. c) Average kinetic energy of the fragments but the largest. d) Oxygen c.m energy spectrum. The calculated oxygen spectra with (grey) and without (line) collective radial motion have been normalized to the data.

Fig. 3. Average c.m kinetic energy of the light charged particles (black points) for a perpendicular emission ($70° \leq \Theta_{cm} \leq 110°$). The result of the calculation which reproduces the associated fragment characteristics ($< E_r >$=2 A.MeV) is shown (grey points).

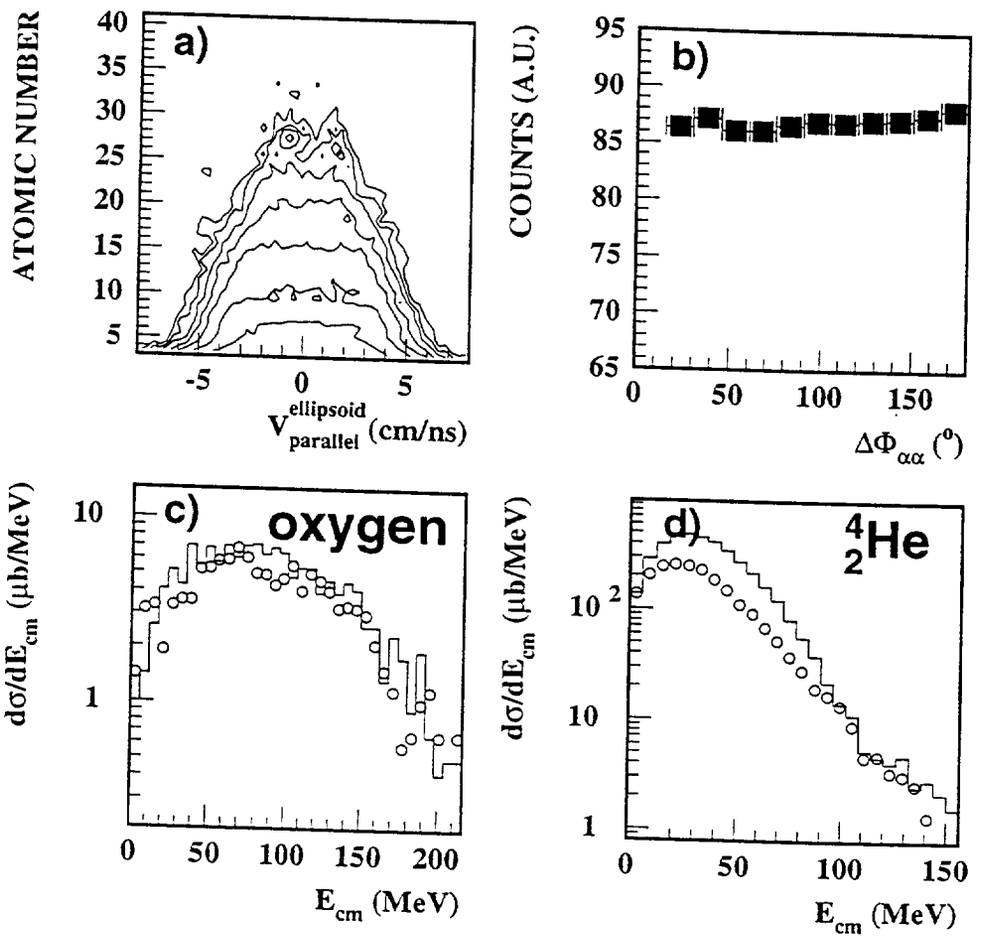
a)
ATOMIC NUMBER
40
35
30
25
20
15
10
5
-5
0
5
$V^{ellipsoid}_{parallel}$ (cm/ns)
b)
COUNTS (A.U.)
95
90
85
80
75
70
65
0
50
100
150
$\Delta\Phi_{\alpha\alpha}$ (^{o})
c)
oxygen
$d\sigma/dE_{cm}$ (μb/MeV)
10
1
0
50
100
150
200
E_{cm} (MeV)
d)
$^4_2$He
$d\sigma/dE_{cm}$ (μb/MeV)
10^2
10
1
0
50
100
150
E_{cm} (MeV)

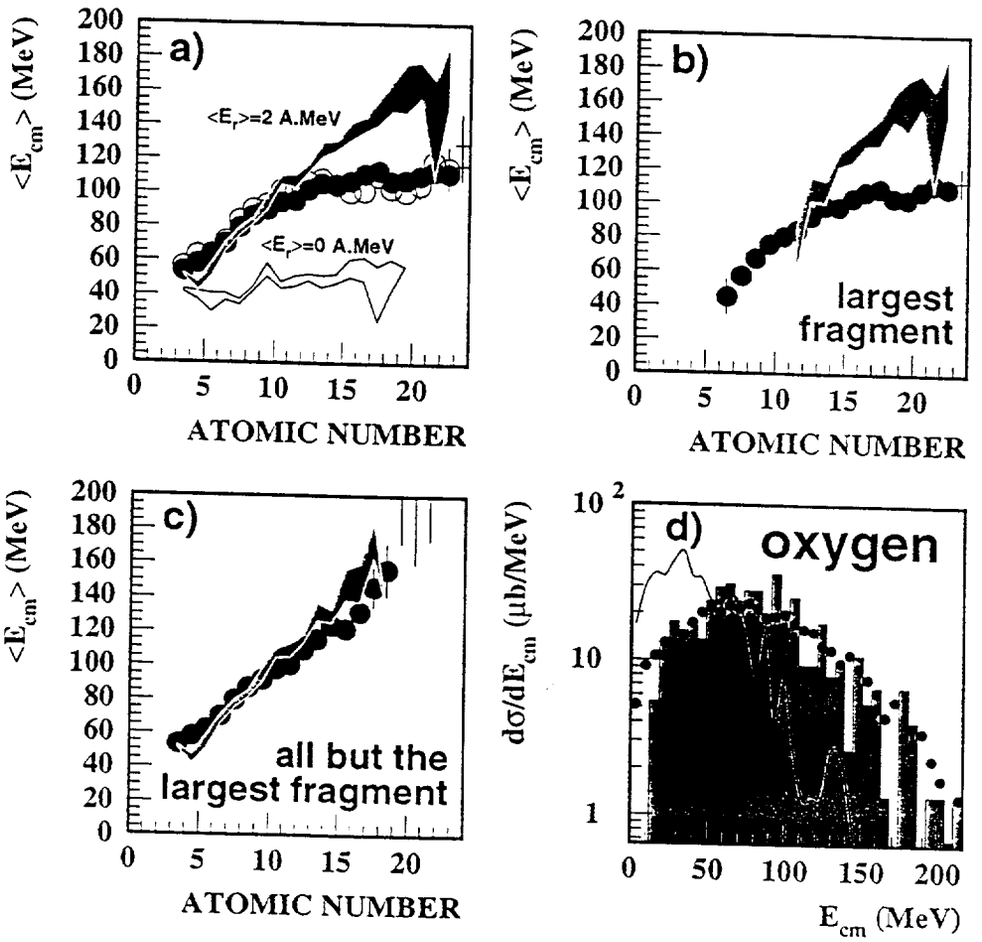
a)
<E_r>=2 A.MeV
<E_r>=0 A.MeV
<E_cm> (MeV)
ATOMIC NUMBER
b)
largest fragment
c)
all but the largest fragment
d)
oxygen
dσ/dE_cm (μb/MeV)
E_cm (MeV)

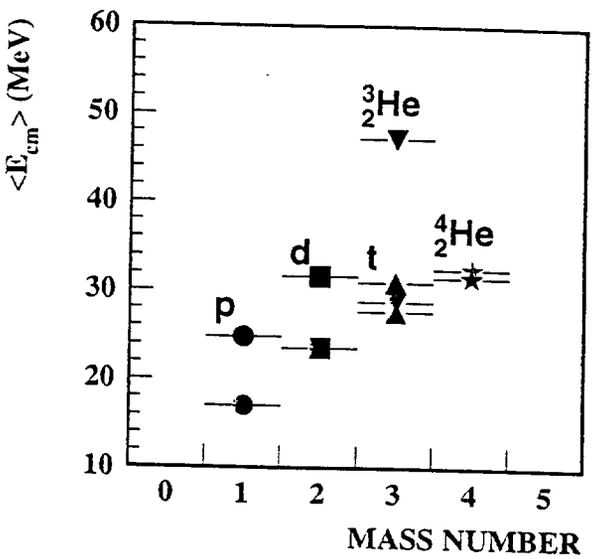
60
50
40
30
20
10
<E_cm> (MeV)
0
1
2
3
4
5
MASS NUMBER
3 2He
4 2He
d
t
p